Power Allocation Influence on Energy Consumption of a Double-Ended Ferry

Daniel Vergara[1], Martin Alexandersson[1,2], Xiao Lang[1], Mao Wengang[1]
[1]Dept. of Mechanics and Maritime Sciences, Chalmers University of Technology
[2]RISE Sweden AB,
Gothenburg, Sweden

ABSTRACT

Fuel is one of the highest cost items while operating a ship, and its combustion results in air emissions polluting environments. Finding ways to increase shipping operations efficiency without compromising the provided service quality is necessary for economic and environmental reasons. This study first used data analysis to find hidden information in one-year navigation data of a double-ended ferry operated along the Swedish coast. The case study ferry was operated using both bow and stern engines partly loaded. A new feature of the power ratio is defined to describe the influence of engine power allocation on total fuel consumption. Then, different machine learning methods are used to establish the ship's total fuel consumption model due to influences of external factors such as wind and sea currents, etc., together with the power ratio. The established machine learning model is used to find the most efficient operation of allocating power to different engines. It shows that, in theory, up to 35% fuel savings can be achieved for the case study vessel. These findings can further aid with the operational planning for the scope of Eco-driving.

KEY WORDS: Energy efficiency; machine learning; exploratory data analysis; XGBoost; double-ended ferry

INTRODUCTION

Double-ended ferries are an alternative to bridges or tunnels for transporting passengers and cars over water. They are used for commuting in big cities like New York (Siferry 2022), London (TRL 2022), and connecting islands along the coast. Double-ended ferries can achieve this task on short routes where maneuverability may be difficult (Waterhouse, 2016), and relieve road congestion (Leung et al., 2017). The objective in maritime transport is to reduce CO_2 emissions by at least 40% by 2030 and to pursue efforts to reach 70% reduction by 2050, compared to the 2008 setup by IMO (2018). Maritime authorities also push regional ferries to become more environmentally friendly and save fuel costs. It becomes important to investigate how to operate these vessels to reduce energy consumption. For this purpose, a fundamental problem is establishing a reliable performance model to describe those ferries' fuel consumption in terms of their operational profiles, such as allocation of engine load, ship speed, etc. Different models have been researched in the maritime community to address this problem.

Empirical formulas are often used to determine a ship's resistance from the ship type and dimensions. For example, those developed by Holtrop and Mennen (1982) or Hollenbach (1998) are often used to predict how much power is required. They are well suitable for ship design purposes, but do not consider operational factors and dynamics that should be optimised in a vessel operation. Alternatively, computational fluid dynamic simulations can predict resistance and power, but they need high computational effort (Carlton, 2007). Nowadays, data driven strategies have been widely investigated for predicting energy demand in ships by using recorded measurements and operational data. Digitalization in the shipping industry has led to large amounts of data collected that can be used to improve ships' energy performance. Examples of this can be found in Blueflow (2022) and YaraMarine (2022), which aim to promote eco-driving by exploiting hidden trends inside the data.

Data driven methods often rely on statistical (Mao et al., 2016) or supervised machine learning methods (Lang et al., 2022) to build models describing ship energy performance. These methods are fast, and their reliability lies in the quality and amount of the data (Corrales et al., 2018). Making the best use of these large quantities of data allows for determining data driven strategies from data information. The data driven models using decision Trees (Laurie et al., 2021) and Artificial Neural Networks (Karagiannidis and Themelis, 2021) have proven useful in predicting power demand and energy consumption of ships (Zhang et al., 2019).

Therefore, this paper aims to investigate the optimal allocation of engine/propeller operations for the double-ended case study ferry. First, a machine learning framework is developed to model the ferry's fuel consumption in terms of its operational parameters and encountered

ocean environmental parameters. Based on the established machine learning model, how to reduce energy consumption (fuel consumption) is investigated by evaluating the impact of the ferry's total fuel consumption for simulating different power allocations between the bow and stern engines. Details on how the simulator works and how the models were defined are also presented.

PRINCPLES OF SHIP PROPULSIONS

Internal combustion engines (ICE) and screw propellers are the most common propulsion system in ships (Latarche, 2021). The advantages of ICE lie in their capability compared to alternative propulsion systems in long-distance travel (Farnsworth, 2022). In the case of double-ended ferries, they operate by having a symmetrical configuration with two main engines located at the bow and stern of the ship. It allows a return trip by switching the main engine without turning the ship (Waterhouse, 2016). However, the leading physics of each of these main engines remains the same as for regular ICE. First, the power delivered from propeller to water, also named thrust power P_T, is defined as:

$$P_T = T \cdot V_A = T \cdot V_w \cdot (1 - w) \quad (1)$$

where the thrust force T generated from the propeller is used to push the ship forward, corresponding to the velocity of arriving water at the propeller (also known as the speed of advance of propellers) V_A. The thrust force can move the ship with a specific speed through water V_w. The difference between propeller advanced speed and ship forward speed is caused by the wake velocity induced by the friction along a ship's hull surface. The wake fraction coefficient w quantifies it in Eq. 1. In addition, the rotation of propellers can cause the water in front of the propeller to be "sucked" back to the propeller, leading to extra resistance on a ship's hull as follows:

$$R_T = T \cdot (1 - t) \quad (2)$$

where R_T is the total ship resistance with speed through water V_w, and t is the thrust deduction coefficient. The hull efficiency is defined as:

$$\eta_H = \frac{P_E}{P_T} = \frac{T \cdot (1-t) \cdot V_w}{T \cdot V_w \cdot (1-w)} = \frac{1-t}{1-w} \quad (3)$$

where P_E is the effective power. If the speed through water V_w is not known, it can be estimated by the speed over ground V_g as:

$$V_w = V_g + V_{sc} \quad (4)$$

where V_{sc} is the sea current speed along the ship's sailing direction. The fuel consumption of the required thrust engine power is estimated by:

$$m_{\text{fuel}} = \frac{SFOC \cdot P_T}{\eta_o \eta_R \eta_s} \quad (5)$$

where η_o, η_R, η_s represent the open propeller efficiency, relative rotative efficiency, and shaft efficiency, respectively, while *SFOC* is the specific fuel oil consumption. The propeller efficiency and *SFOC* depend strongly on the ship engine loads, and engine rotation speed. How to allocate engine loads on each propeller will greatly impact a ship's total fuel consumption. From the above equations, it should also be noted that the shape of the ship hull and where the propeller is located along the hull will significantly impact the hull efficiency and the total fuel consumption. Therefore, optimization of power allocation between the bow and stern propellers should reduce total fuel consumption for the double-ended ferries.

CASE STUDY FERRY

Double-ended ferries have the characteristic that they have one propeller located at the bow and one at the stern. It allows for a particular energy optimization method, i.e., engine power allocation. One year of data from Uraniborg (Rederi AB Ventrafiken), a double-ended ferry presented in Fig. 1, was available for this case study. The measurements were used in this study to find out which strategy for allocating engine power could save fuel. The ferry has two symmetric azimuthal propellers driven by identical ICE Caterpillar C32 ACERT V12, each with 709 kW and 1600 rpm. The installed engine load specification is presented in Fig. 2. For this case study vessel, the actual power at each engine is given as the engine load ratio ξ in percentage, corresponding to the maxima engine power. Thereafter, the actual engine power can be calculated by:

$$P = P_{max}(N) \cdot \xi \quad (6)$$

where P_{max} is the maximum engine power for a given engine rotation speed n, as presented in the black line on top of Fig. 2. For the two installed Caterpillar engines, their engine load ratios are collected through the engine management system, and the ratios ξ can be used to estimate the engine power as in Eq. 6.

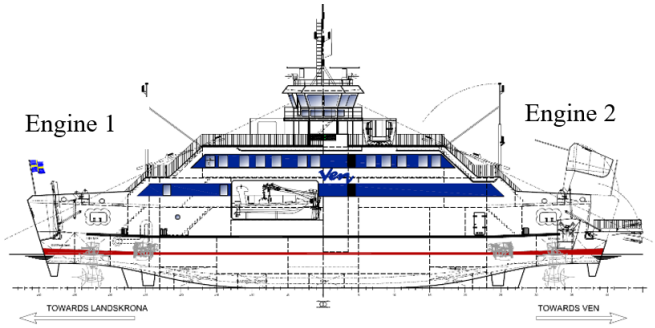

Fig. 1. The case study double ended Ropax ferry "Uraniborg".

As this ship is symmetric the ship's bow will be considered to be always in the sailing direction and consequently changing position between eastbound and westbound trips. For example, on westbound trips Engine 1 will correspond to the stern engine and Engine 2 to the bow engine.

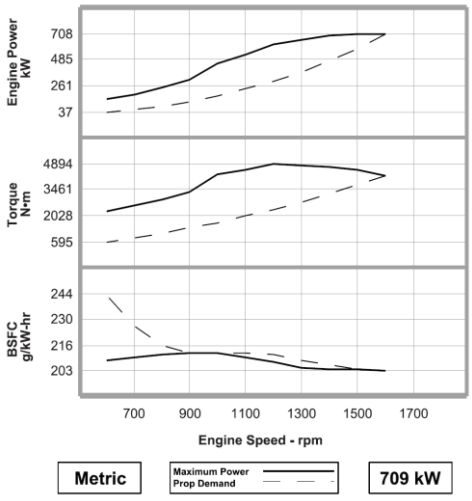

Fig. 2. Engine curves of the installed engines (Caterpillar, 2009).

DATA ACQUISITION AND PROCESSING

The double-ended ferry has onboard an energy management system that records operational data according to ISO 19030-2016 (ISO 2016). In addition to the engine load ratios ξ, the data comprises 24 different features corresponding to both seakeeping, operation, and engine power related parameters, such as locations, speed over ground V_g, engine brake power P, and fuel consumption rate m_{fuel} at both bow and stern engines, etc. The data collected for this analysis corresponds to one year of operations from January 2021 to January 2022.

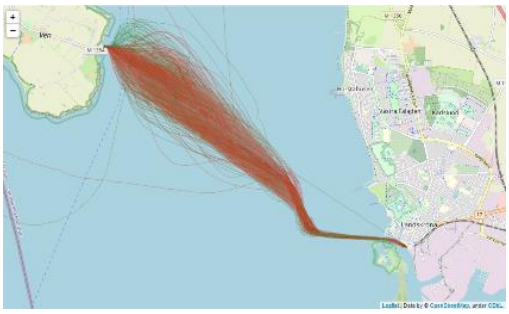

Fig. 3. Sailing trajectories between Ven and Landskrona for the case study ferry from 2021-01 until 2022-01.

The ferry travels between Landskrona and Ven in 9 return trips (18 total) per day. The route is fixed, and its length is approximately 4 nautical miles. The sailing routes during this one-year operation are shown in Fig. 3. In order to consider the weather impact on the ferry's fuel consumption, the wind speed and wind direction encountered by the ferry are extracted from the ERA5 reanalysis database (Copernicus, 2022). The sea current is obtained from the Copernicus Marine Service (Copernicus, 2022). The speed thourgh water is estimated by the ISO guidelines from the measured V_g.

All recorded trips were divided into eastbound (Ven to Landskrona) and westbound (Landskrona to Ven) based on the sailing direction. Each trip is uniquely defined by its velocity profile, as in Fig. 4, with the following characteristics:

- the ferry starts from zero speed until reaching service speed, named as the acceleration phase of about 5 minutes,
- then, the ferry sails with stable service speed, named as cruise phase,
- finally, the ferry deaccelerates from service speed to zero speed, named the deacceleration phase of about 4 minutes.

The typical transit time is about 30-35 minutes. It should be noted that only the ship performance data collected during the cruise phase are of interest in this study since the ferry is in stable and equilibrium conditions.

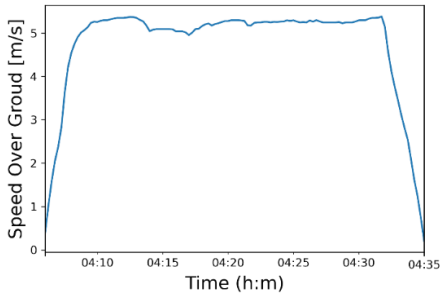

Fig. 4. Ferry speed over ground profile during a case study trip, including acceleration phase, cruise phase, till deceleration phase.

A dataset containing the macro statistics from each trip was created from the original dataset. Following a standard data analytics approach, the data was cleaned and elaborated to improve the resolution of the predictions. For example, due to the richness of the provided dataset, some missing/error measurements were removed. The cleaning algorithm proposed by Karagiannidis and Themelis (2021) is used to identify data outliers.

POWER ALLOCATION INFLUENCE ON FUEL CONSUMPTION

Due to the wake velocity generated by the ship hull when advancing, the propulsive efficiency of the stern propeller, in theory, should be higher than the bow propeller (Lars & Hoyte, 2010). Dependent on the optimal engine load and capacity of each design engine power for propulsion, the *SFOC* may have some counteractive effect for using the stern propeller on total fuel consumption. Therefore, studying the optimal allocation of power between the bow and stern engines is worthwhile. First, a new operational variable power ratio R_P is defined as follows:

$$R_P = \frac{P_{\text{stern}}}{P_{\text{bow}}+P_{\text{stern}}} \tag{7}$$

where P_{stern} and P_{bow} represent the engine power at the stern and bow engines, respectively. It should be noted that the definition of bow and stern is based on the ferry's sailing directions and the actual engines switch between eastbound and westbound trips. This new feature is bounded in the range [0,1] and indicates how much power output comes from either engine. $R_P = 0$ means all power comes from the bow engine and $R_P = 1$ presents all power and thrust is coming from the stern engine. For the individual trip, the average power ratio is computed by:

$$\overline{R_P} = \frac{1}{n}\sum_{i=1}^{n} R_P^{(i)} \tag{8}$$

where n is denoted as the total number of measurement points in one trip, and the measurement frequency is Δt = 15 seconds. Then, the total fuel consumption during a trip is calculated by:

$$M = \sum_{i=1}^{n} m_{\text{fuel}}^{(i)} \cdot \Delta t \tag{9}$$

where m_{fuel} is the fuel consumption rate as defined in Eq. 5.

The data mining analysis will be first performed to study the influence of power ratio R_P on the ship's total fuel consumption for different individual trips. It aims to find the possible trend and inference of engine power allocation with fuel consumption. Then, various machine learning methods will be used to establish a model that can describe the ship's total fuel consumption (per voyage) in terms of her speed, two engine loads, and especially the engine power ratio. Finally, the total fuel consumption at different engine power allocations is simulated by the optimal R_P to verify the energy efficiency improvement.

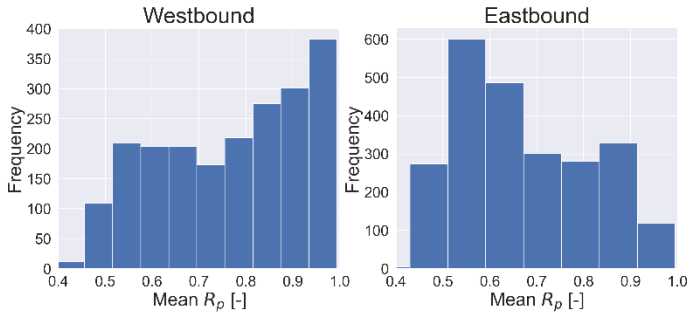

Fig. 5 Frequency distribution of the mean power ratio for one-year data. (left: westbound; right: eastbound)

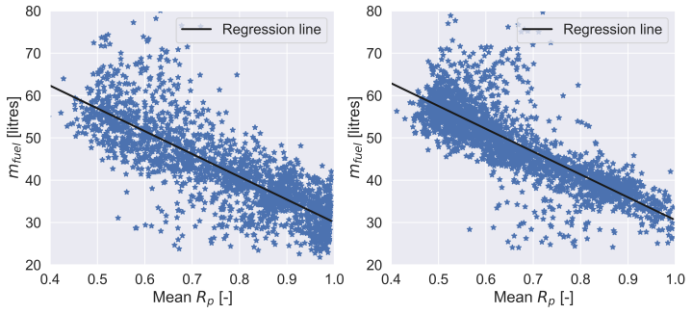

Fig. 6. Fuel consumption versus mean power ratio of each trip for one-year data. Notice the sharp trend toward using only the stern engine. (Left: westbound; right: eastbound)

A frequency distribution histogram of the mean power ratio along westbound and eastbound trips can be found in Fig. 5. A large amount of the operations for the case study ferry are carried at a medium range R_P. This is especially true for eastbound trips and not necessarily the case for westbound trips, which are less constrained with their timetables. The total fuel consumption for each trip was computed and presented in each direction in Fig. 6. The plots show a clear negative slope toward increasing the trip average power ratio. These plots indicate that using the stern-most propeller can be a more efficient way to operate the case study double-ended ferry.

MACHINE LEARNING MODELLING

Input Features

To build a model to describe the ferry's fuel consumption in terms of the so-called engine power ratio R_P, other features that affect the ferry's sailing performance and fuel consumption are also necessary to be considered in the model. The other features include, for example, the northward and eastward wind velocity U_{wind}, V_{wind}, current velocity U_{current}, V_{current}, ship speed over ground V_g, stern engine speed and bow engine speed denoted by n_{stern} and n_{bow}. Three machine learning algorithms are used to establish the model: polynomial regression, artificial neural network (ANN), and XGBoost. For the modeling, the data of those features were normalised using the min-max scaling method, which brings all data to a [0, 1] range.

It is known that the ship's fuel consumption is proportional to the cubic power of the ship's speed through water. The model is then fitted with the so-called polynomial features, and the least-squares method is used to regress all the coefficients in the polynomial model. Similarly, the fuel consumption model was also formulated using different machine learning models to see the influence of not only the power ratio but also the MetOcean conditions as follows:

$$m_{\text{fuel}} = f\left(V_g, U_{\text{wind}}, V_{\text{wind}}, U_{\text{current}}, V_{\text{current}}, R_P, n_{\text{stern}}, n_{\text{bow}}\right) \quad (10)$$

Using the features and the training strategy mentioned above, machine learning models (XGBoost, ANN) were created and assembled in a way that allowed for the simulation of the ferry's total fuel consumption.

Hyperparameter Tuning

Each model was then tested individually for its performance on the test set. The evaluation metric is the coefficient of determination (R^2). Another metric used is the mean squared error (*MSE*). The models were trained using 80% of the data chronologically as the train set, and the subsequent 10% of the data as the validation set to optimal hyperparameters. The remaining 10% is the test set for the fuel consumption prediction in future unseen trips. Hyperparameters configure the settings of the model and cannot be estimated a priori before training (Yang and Shami, 2020). A randomised search was carried out to tune these hyperparameters systematically to improve the model metrics results using the data on the validation set.

As the default settings for neural networks and XGBoost had similar performance, XGBoost was chosen as the best method due to the modeling efficiency when compared to a neural network. This model was therefore subjected to hyperparameter tuning using a randomised search with the following parameters:

- Max depth: (3, 5, 10)
- Learning rate: (0.01, 0.1, 0.2, 0.3)
- Sub-sample: 0.5 to 1 (0.1 intervals)
- Column sample by tree and level: 0.4 to 1 (0.1 intervals)
- Number of estimators: 100 to 200 (20 intervals)
- Number of iterations 25

RESULTS AND DISCUSSION

Evaluation of regression models from filtered data yields that they have similar performance, as shown in Fig. 7. All the regression models seem to follow the same trend in the predictions. The models tend to overestimate the fuel consumption, especially with fuel consumptions in the range between 100 and 140 l/h. This misfit is expected since - in general - regression models are not perfect and in practice signals are subject to noise and perturbances that affect their behaviour.

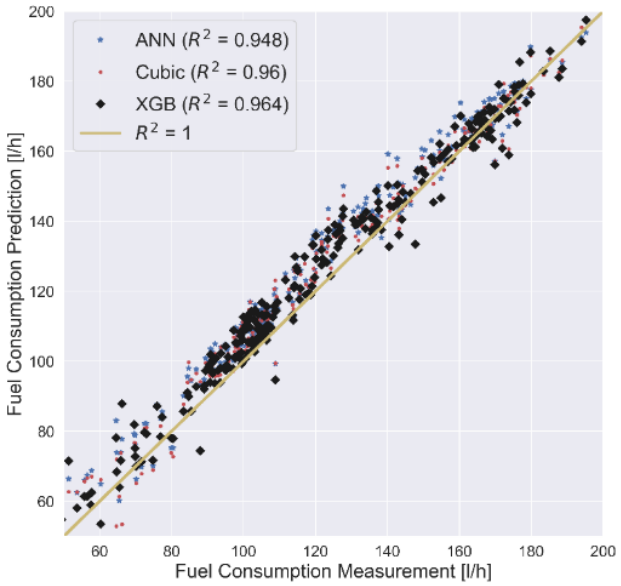

Fig. 7. Performance prediction of the different machine learning models on test set. The data was taken at regular 30 min intervals from the regression results for better visualization.

To make a more detailed evaluation how each model performs on individual voyages, two trips from the test set were evaluated – one westbound and one eastbound trip. Fig. 8 shows the goodness of fit of the predictions with the different regression models for the westbound trip. Fig. 9 shows the same thing for the Eastbound trip. It can be seen how locally the different regression models perform with all of them having a similar performance on the chosen trips. The XGBoost regression model has a slightly better performance on the Eastbound trip.

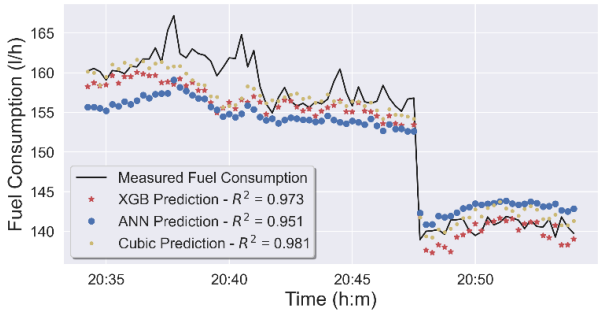

Fig. 8. Comparison of fuel consumption prediction by different models on a 2021-11-25 westbound trip in time series.

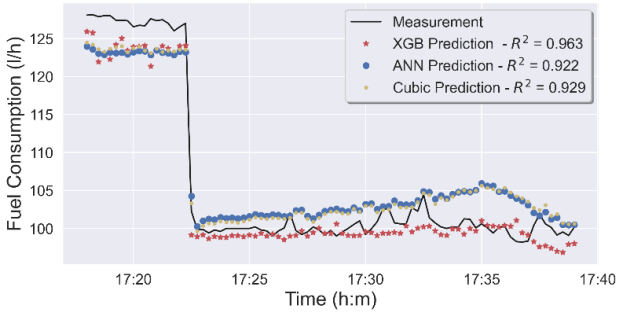

Fig. 9. Comparison of fuel consumption prediction by different models on a 2021-11-25 eastbound trip in time series.

Based on the goodness of fit, the XGBoost was chosen for fuel consumption predictions. An advantage of the XGBoost regression algorithm is that it provides a feature score. This feature score indicates how important each input features on the final prediction. The higher the score, the higher the importance of the feature. Furthermore, delving into XGBoost feature importance, it was noticed that R_P, n_{stern}, and n_{bow} had the highest impact on the fuel prediction as shown in Fig. 10. From Eq. 6, it follows that the power is a function of the engine speed, while Eq. 5 shows that the total fuel consumption is a function of the propulsion power. These factors are reflected in the high feature score that the engine speed presents. Furthermore, the input feature R_P is very important for the model predictions.

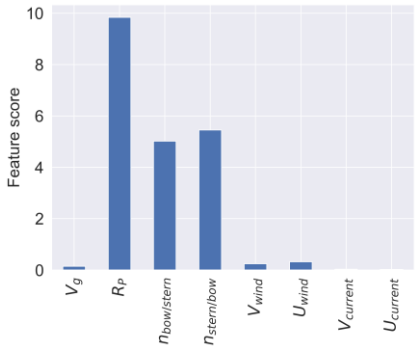

Fig. 10. The feature importance ranked for the XGBoost-based fuel consumption prediction model.

Another indicator of the regression goodness comes from its accuracy in predicting the total fuel consumption, which was computed by Eq. 8. The prediction error ϵ was determined as:

$$\epsilon = \frac{M_{\text{XGB}} - M_{fuel}}{M_{\text{fuel}}} \quad (11)$$

The kernel density of the prediction error was determined and plotted in Fig. 11. The errors were normally distributed, with 83% of the error distribution lying in the range $\pm 2\epsilon$ and 96% within the range $\pm 4\epsilon$.

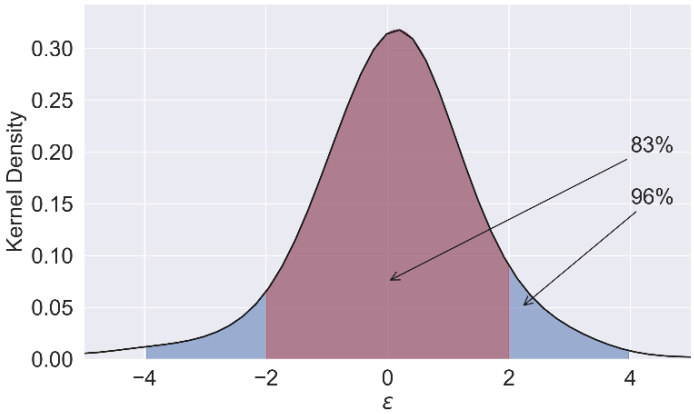

Fig. 11. Kernel density estimation (KDE) of the prediction error.

SIMULATION OF DIFFERENT POWER RATIO ALLOCATION

The model requires logical inputs to describe the engine performance at different power ratio allocations, since the machine learning model may produce unreasonable output when inputting unrealistic values. The data were first filtered such that the mean V_g was fixed around 5 m/s ±2%. Fig. 12 shows a heatmap of the joint distribution of R_P and V_g. This allows determining the most realitic values of R_P. As shown in Fig 12, a wide range of R_p can achieve the target speed, and these values exist in the dataset. Thus, different power ratios, ranging from 0.4 to 1, can be selected.

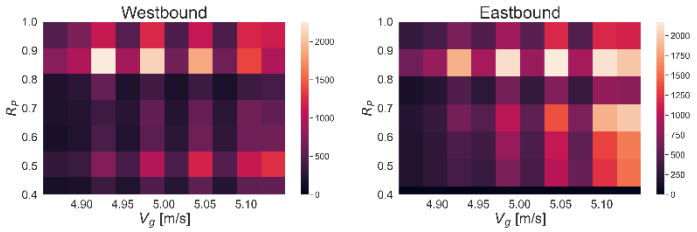

Fig. 12. Heatmap of the joint distribution of R_P and V_g.

After an R_P value was selected, the joint distribution of N_{stern} and N_{bow} was plotted for specific range, i.e., *target*(R_P) ±0.01, as shown as example in Fig. 13 for $R_P = 0.7$. This filter returns the most frequent combination of N_{stern} and N_{bow} for said R_P.

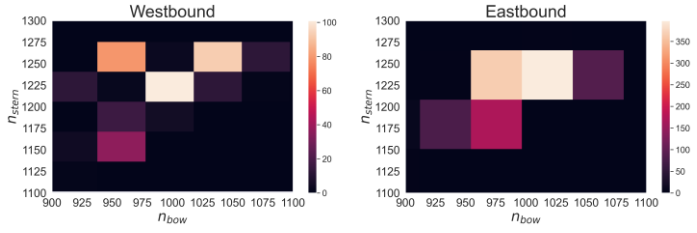

Fig. 13. Heatmap of the joint distribution of N_{stern}, and N_{bow} in the range R_P = 0.69 to 0.71. The box with the highest frequency was chosen to approximate the operation conditions with highest probability.

In this study, the two case study voyages in Fig. 8 and Fig. 9 were also selected to simulate the fuel consumption for different power ratio conditions respect to the initial average conditions already presented in the measurements listed in Table 1. As seen in figure 8 and 9 the selected trips show a step-like behaviour. This splits the trips into two identifiable regions at approximately constant R_P.

Table 1. Description of the case study trips measurements

		1st Region			2nd Region		
Voyage	$\bar{V}_g$	$\bar{R}_P$	$\bar{n}_{\text{stern}}$	$\bar{n}_{\text{bow}}$	$\bar{R}_P$	$\bar{n}_{\text{stern}}$	$\bar{n}_{\text{bow}}$
Westbound	5.1	0.48	1230	1238	0.53	1198	1159
Eastbound	4.9	0.62	1213	986	0.89	1230	787

The selected simulation parameters are listed in Table 2 and the simulation results are presented in Fig. 13 and 14, respectively. It should be noted that although the power ratio and engine speed vary, the travel time is approximately the same (ETA 45s difference).

Table 2. Simulation parameters for the two case study voyages.

Voyage	$\bar{V}_g$	R_P	n_{stern}	n_{bow}
Westbound	5	1	1250	600
	5	0.7	1225	1000
	5	0.4	1210	1270
Eastbound	5	1	1200	600
	5	0.7	1250	1025
	5	0.5	1240	1225

It should also be noted that the power ratio during the voyages is not constant as indicated by the arrows in Fig. 8 and Fig. 9 and represented with a jump in fuel consumption. The reason for this behaviour being that the current operation mode has no consideration for R_P. This data is still considered part of the steady state condition of the voyage.

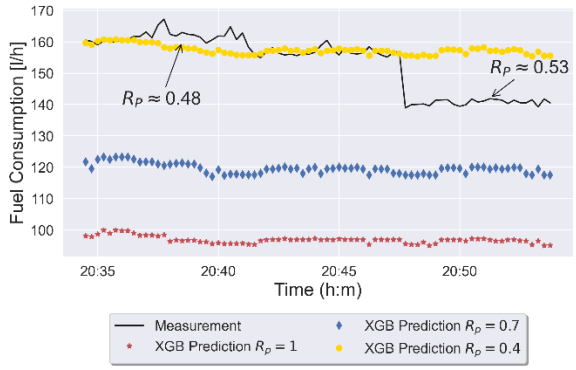

Fig. 14. Simulation of the fuel consumption on the case study westbound trip using the conditions from Table 2.

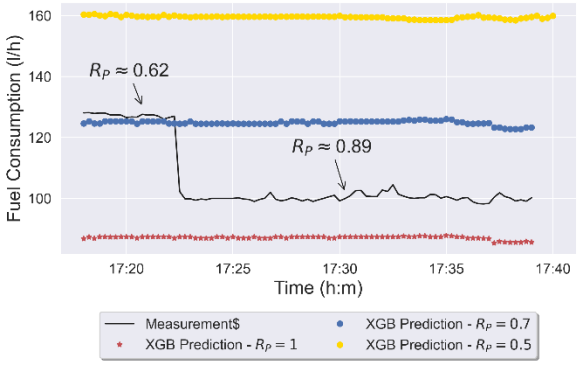

Fig. 15. Simulation of the fuel consumption on the case study eastbound trip using the conditions from Table 2.

For the simulations of the two case study voyages, the power ratio R_P = 1 has achieved the lowest fuel consumption in operation and as shown in the figures, as the power ratio decrease, the fuel consumption increase. It can be noted from the measured data itself that the regions with higher R_P correspond with lower fuel consumption. This observation follows the trends presented in Fig. 6.

Applying Eq. 8 to predict the total fuel consumption, which was determined by simulating the operation by proposed operational conditions in Table 2 when R_P = 1. The measured fuel consumption per voyage and the simulated fuel consumption are presented in Table 3.

Table 3. Summary of the selected simulation results

	Measured M_{fuel} (litres)	Simulated M_{fuel} (litres)	Saving
Westbound	54.90	34.72	35.8%
Eastbound	41.36	35.5	18.45%

It evident from the simulation that the optimised setup for both trips have a similar expected fuel consumption but that the relative savings are lower for the Eastbound trip. The reason for this lower metric is that the measured M_{fuel} for the Westbound trip is 33% higher than that of the Eastbound trip. A possible explanation for this phenomenon comes from Table 1 as the Westbound trip has a speed on the highest boundary of the filter (5 m/s +2%) while the Eastbound trips lies in the lowest boundary (5 m/s - 2%). If a quadratic relationship between fuel and speed is assumed:

$$M_{\text{fuel}} \propto \bar{V}_g^2 \tag{12}$$

Then the Eastbound trip would approximately have 7.7% lower fuel consumption. Furthermore, from table 1 the different $\bar{R}_P$ are show, corresponding to different parts of the trip. From figure 6 a simple analysis shows that curves follow a trend given by the lines:

$$\begin{cases} M_{west} = 83.87 - 53.834 \cdot R_P \\ M_{east} = 84.455 - 53.888 \cdot R_P \end{cases} \tag{13}$$

So, in average a westbound trip with $R_P = 0.53$ should have a consumption of 55.3 litres and a trip with $R_P = 0.89$ a consumption of 35.95 litres, or a 35% lower consumption, assuming that they both have similar conditions. A combination of these two factors, lower speed and higher power allocation, may be the reason behind this difference.

The simulation on the optimised setup using the machine learning models however how that around 35% and 18% fuel savings could be achieved. It shows that once enough data is collected from these tests, it can be analysed to further insight into the possible energy savings using this operation. A proposal was submitted to the transport company to evaluate the effect of this power ration allocation.

CONCLUSIONS

Data mining techniques have been implemented in this study to find trends in fuel consumption in terms of two engines power allocation for a double-ended ferry. It was shown from this exploratory analysis that operation mainly on the stern engine is a more efficient way to operate the case study ferry.

Then different machine learning algorithms were used to model the relationships between fuel consumption, engine parameters, and weather conditions. The best performed XGBoost model is chosen to simulate different power allocation conditions for total fuel consumption estimation of two case study voyages. It was found that up to 35% fuel saving can be achieved in theory compared to the actual measurements. The optimised operation has been reported to the ferry company for demonstration experiments. A more thorough comparison between the theoretical simulation and experiments will be conducted in the next stage study.

ACKNOWLEDGEMENTS

The authors acknowledge the financial support from the Vinnova project 2021-02768, and Energimyndigheten (Swedish Engery Agency) project Data-driven energy efficiency of ships (project: 49301-1) for providing the resources to prepare this paper. Also special thanks to Ventrafiken for providing the data that allowed for these analyses.

REFERENCES

Blueflow (2022). Products - Blueflow Energy Management AB. https://www.blueflow.se/products/ Retrieved October 2022.

Borgnakke, C., Sonntag, C., & Van Wylen, G. J. (2003). Fundamentals Of Thermodynamics (Sixth). Wiley.

Carlton, J. S. (2007). Marine Propellers and Propulsion (Second). Butterworth-Heinemann.

Catepillar (2009), C32 ACERT™ MARINE PROPULSION - 1015 mhp (1000 bhp) 746 bkW.

Copernicus Climate Data Store |. (2022). Retrieved 20 September 2022, from https://cds.climate.copernicus.eu/

Corrales, D., Corrales, J., & Ledezma, A. (2018). How to Address the Data Quality Issues in Regression Models: A Guided Process for Data Cleaning. Symmetry, 10(4), 99. https://doi.org/10.3390/sym10040099

Farnsworth, A. (2022). Long live the internal combustion engine. Retrieved 16 September 2022, from https://www.wartsila.com/insights/article/long-live-the-internal-combustion-engine

Gerr, D. (2001). Understanding Engine Performance. In Propeller Handbook: The complete reference for choosing, installing, and understanding boat propellers (pp. 1–9). essay, International Marine.

Hollenbach K.U. (1998) Estimating Resistance and Propulsion for Single Screw and Twin-Screw Ships. Ship Technology Research 45/2

Holtrop J., Mennen G.G.J. (1982) An Approximate Power Prediction Method. International Shipbuilding Progress, 29, 335, 166–170

International Organization for Standardization. (2016). Ships and marine technology —Measurement of changes in hull and propeller performance — Part 2: Default method (ISO/DIS Standard No. ISO 19030-2:2016(E))

Karagiannidis, P., & Themelis, N. (2021). Data-driven modelling of ship propulsion and the effect of data pre-processing on the prediction of ship fuel consumption and speed loss. Ocean Engineering, 222, 108616. https://doi.org/10.1016/j.oceaneng.2021.108616

Lang, X., Wu, D., & Mao, W. (2022). Comparison of supervised machine learning methods to predict ship propulsion power at sea. Ocean Engineering, 245, 110387.

Larsson, L., & Raven, H. (2010). The Principles of Naval Architecture Series—Ship Resistance and Flow. (1st ed.). The Society of Naval Architects and Marine Engineers (SNAME).

Latarche, M. (2021). Pounder's Marine Diesel Engines and Gas Turbines (Tenth, pp. 13–58). Butterworth-Heinemann.

Laurie, A., Anderlini, E., Dietz, J., & Thomas, G. (2021). Machine learning for shaft power prediction and analysis of fouling related performance deterioration. Ocean Engineering, 234, 108886.

Leung, A., Tanko, M., Burke, M., & Shui, C. S. (2017). Bridges, tunnels, and ferries: Connectivity, transport, and the future of Hong Kong's outlying islands. Island Studies Journal, 22.

Mao, W., Rychlik, I., Wallin, J., & Storhaug, G. (2016). Statistical models for the speed prediction of a container ship. Ocean Engineering, 126, 152–162. https://doi.org/10.1016/j.oceaneng.2016.08.033

Siferry (2022). The Staten Island Ferry https://www.siferry.com. Retrieved October 2022.

TFL (2022). Transport for London: River. https://tfl.gov.uk/modes/river/ Retrieved October 2022.

Waterhouse J. (2016). Fifty plus years of double-ended ferry design. Marine Log. Elliott Bay Design Group.

YaraMarine. (2022). FuelOpt™: A smart way to derate engine power output and meet EEXI requirements – https://leanmarine.com/2021/03/29/fuelopt-a-smart-way-to-derate-engine-power-output-and-meet-eexi-requirements, Retrieved Oct. 2022.